JOURNAL OF PROPULSION AND POWER
Vol. 26, No. 4, July–August 2010

Technical Notes

Study of Detonation Interactions Inside a Two-Dimensional Ejector Using Detonation Transmission Tubing

H. Zare-Behtash,* N. Gongora-Orozco,† and K. Kontis‡
University of Manchester,
Manchester, England M60 1QD, United Kingdom
and
G. Jagadeesh§
Indian Institute of Science, Bangalore 560 012, India

DOI: 10.2514/1.44338

I. Introduction

STUDIES into the diffraction of detonation waves have been motivated not only by the need to suppress accidental detonations but also in the interest of the applicability of such flows to the concept of pulse detonation engines (PDEs). PDEs are currently being investigated as a new technology for aerospace propulsion [1–6]. PDEs are unsteady propulsion devices that produce periodic impulse by using repetitive detonations. Ejectors are fluid pumps that are used to entrain secondary flows using a primary flow. For propulsion applications, this entrainment can augment thrust compared with that generated by the primary flow alone and thereby increase performance [7].

For any given set of flight conditions, there exists ejector inlet and outlet geometries that provide optimal performance [8,9]. Similar to the findings of Kentfield [10], Etele et al. [11] describe the ejector operation envelope as the low- speed low-altitude phases of launch, where the entrainment and subsequent compression of the atmospheric air are largely responsible for any increased performance over traditional rockets. Nonreactive computational studies have highlighted the importance of the starting vortices, precursor shocks, and direct pressure loads created by the gas-dynamic processes within the ejector to the overall thrust-augmentation performance of the system [12,13].

Nonelectrical (NONEL) tubes consist of a polymer tube with a thin explosive coating on the inner wall of the tube. NONEL tubes have been used extensively in blasting and mining, quarrying, crew escape systems in military aircraft, ordnance systems in launch vehicles, and missiles that require the highest functional reliability [14]. A NONEL DynoLine tube was used to generate the shock wave as result of detonation of the reactants inside the plastic tube. According to the system description provided by Orica Mining Services, the velocity of the shock wave through the NONEL tube is approximately 2100 m/s. The present study examines, both qualitatively and quantitatively, the interaction of the resultant flow with a two-dimensional (2-D) nozzle-ejector configuration. The three-dimensional (3-D) effects are confined to the converging section of the nozzle. The analysis is focused on the primary flow features. Therefore, the entrance of the secondary flows through the atria of the nozzle is closed.

Received 12 March 2009; revision received 19 January 2010; accepted for publication 5 February 2010.

*Research Student, School of Mechanical, Aerospace, and Civil Engineering. Student Member AIAA.
†Research Student, School of Mechanical, Aerospace, and Civil Engineering.
‡Professor (Reader), School of Mechanical, Aerospace, and Civil Engineering. Senior Member AIAA.
§Professor, Aerospace Engineering Department. Senior Member AIAA.

II. Experimental Setup

A. Nozzle-Ejector System

The steel nozzle shown in Fig. 1 has a uniform thickness of 19.05 mm, a contraction ratio of 6:1, a throat height of 9.6 mm, and a width of 10 mm [15]. The main objective of the ejector assembly in the study is to make the flowfield as close to 2-D as possible. To ensure this, the ejector assembly consists of two different sections that have been carefully milled with good surface finish and then bolted together ensuring 2-D flow path of the primary flow. The ejector sidewalls become parallel to the centerline at the plane of the nozzle exit with a distance of 45 mm between the upper and lower walls. The total length of the test section was 307 mm with a height of 209 mm. The exits of the lower and upper atria are closed. Overall dimensions of the nozzle are given in Fig. 1a. Optical-grade Perspex sheets with a thickness of 10 mm were used on both sides of the nozzle to allow visualization of the flow. Wall pressure measurements were conducted at the locations marked in Fig. 1b. The data was collected by means of a high-speed data acquisition system (National Instruments PCI-6251). The initial pressure in the test section was ambient. The NONEL tube was flush with the entrance of the nozzle. The signal to begin pressure measurements and image acquisition was obtained via a Kulite XT-190 transducer, horizontally mounted 5 mm from the exit of the NONEL tube, as shown in Fig. 1b.

B. NONEL

The flexible NONEL tube, with an outer diameter of 3 mm and an internal diameter of 1 mm, was inserted into an aluminum hypodermic tube with an internal diameter of 3.28 mm. This ensured that the tube would not be loose during firing and also allow sufficient room to easily change the NONEL tube after each run. 0.9 m of NONEL tubing was used for each run.

The detonation was initiate by an electronic blasting machine, DynoStart 2, with a capacitance of 0.2 μF and an output voltage of 2500 V. Both DynoLine and DynoStart were manufactured by Dyno Nobel Sweden AB (now Orica Mining Services). The DynoLine contains 16 mg/m of octogen (HMX) and 2 mg/m of aluminum powder. When the microexplosive is electrically triggered from one end of the polymer tube, a detonation wave is generated inside the tube. When this detonation front is allowed to escape from the open end of the NONEL, a microblast wave is generated. Since the amount of energy expended in the generation of the blast wave from the open end of the NONEL tube is very small ($\sim$8.7 J; trinitrotoluene equivalent $\sim$1.63 mg), they are referred here as microblast waves.

Preliminary tests were carried out to calculate the velocity and shape of the incident shock wave produced by the NONEL tube with no obstacles. The velocity of the spherical shock wave at a distance of 20 mm was approximately 700 m/s. The average pressure level at a distance of 10 mm from the NONEL was 1.78 bar [16].

C. High-Speed Shadowgraphy

High-speed shadowgraphy [17], with an optical arrangement similar to that used by Kontis et al. [18], was employed to visualize the flow. The Shimadzu Hyper-Vision camera, capable of recording

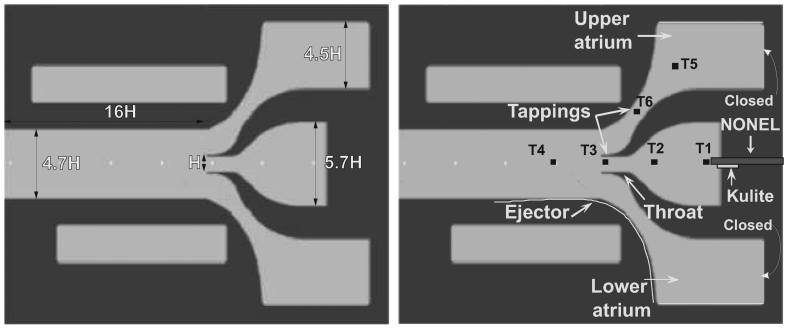

a) b)

Fig. 1 Schematic diagram of the test section: a) overall dimensions (H = 9.6 mm) and b) description.

images at a frame rate of up to 1 megaframe per second with exposure time of 0.50 μs, was used to produce a motion picture consisting of 100 images with spatial resolution of 312 × 260 pixels. Illumination for the Shimadzu camera was provided via a 300 W continuous Xenon lamp.

III. Results and Discussion

Figure 2 shows the average pressure of three test runs triggered by the Kulite transducer. The repeatability of the pressure measurements was calculated as 7%.

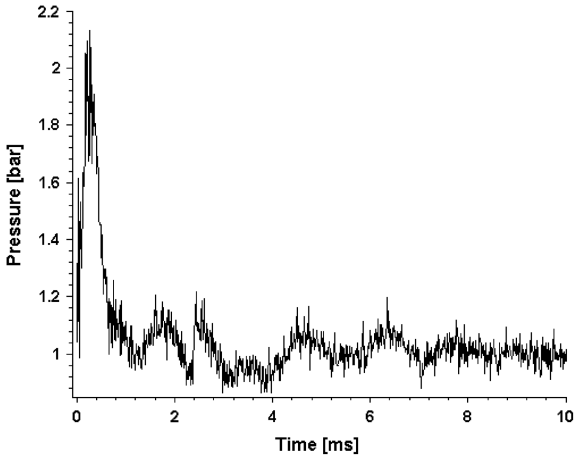

Fig. 2 Pressure trace of triggering transducer.

Figure 3a shows the emergence of the shock front (denoted by S) and the products of combustion (PC) from the NONEL tube placed at the entrance of the test section at the right-hand edge of the image. A triple point (denoted by T) is formed where the reflected shock wave from the sidewall (optical window) merges with the incident shock front. The incident shock reflects from the upper and lower walls of the test section, creating reflected shocks, denoted as R1 and R2 in Fig. 3b. As the incident shock continues through the convergent portion of the nozzle and into the uniform area channel, multiple Mach waves (denoted as m) are visible propagating behind shocks R1 and R2, which are generated from the combustion cloud encased by the same shocks (Fig. 3c). The average velocity of the product of combustion is 200 m/s although initially the velocity is as high as 600 m/s. The subsonic velocity of the product of combustion resemble that of a single jet of hot gases generating disturbance waves or Mach waves.

For each experiment a finite length of the NONEL tube is used, hence in every shock only a finite amount of products of detonation are released. The hollow section (denoted by H) in the middle of the combustion cloud in Fig. 3c forms due to the depletion of the PC exiting the NONEL tube. Although the initial shock wave from the NONEL tube is spherical (3-D), the effects on the flowfield are contained by the contraction of the nozzle.

Shocks R1 and R2 approach each other head on and cross over in Fig. 3d. At the same time the Mach waves appear to coalesce and become stronger (denoted by M) due to the area reduction. Once shocks R1 and R2 have passed each other, they collide with the walls of the test section, in Fig. 3e. After colliding, the shocks (now labeled R1' and R2'), move upstream toward the NONEL tube while the incident shock reaches the end of the uniform area channel. The

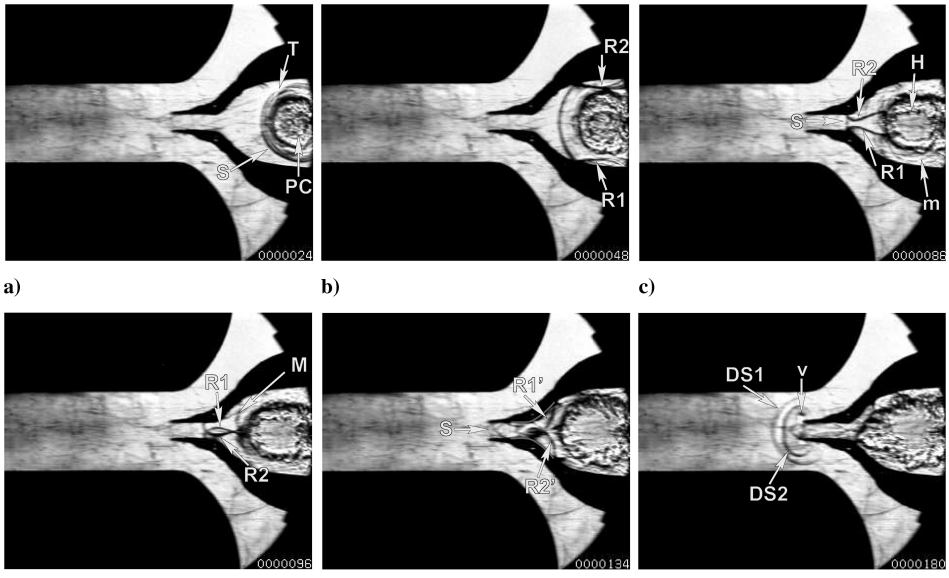

a) b) c)

d) e) f)

Fig. 3 Segment 1 of flow analysis.

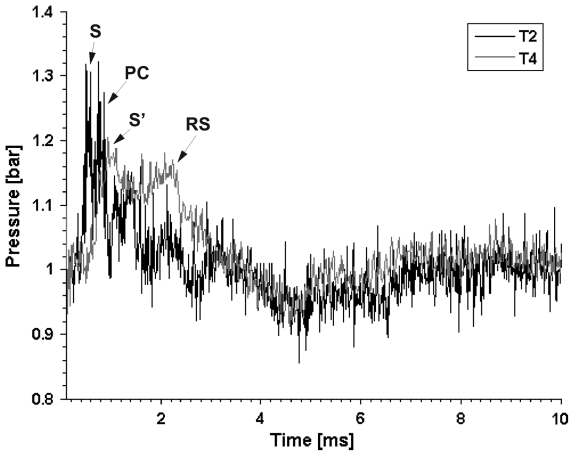

Fig. 4 Pressure history of transducers T2 and T4 (see Fig. 1).

diffraction of the incident shock and the newly formed shock wave from the coalescence of the Mach waves (M in Fig. 3d) generate two diffracted shocks (DS1 and DS2), as well as two vortex cores (denoted as v), due to the roll up of the shear layer between the emerging and ambient fluid in Fig. 3f.

Figure 4 shows the pressure traces of transducers T2 and T4 (see Fig. 1 for locations). Transducer 2 shows two distinct peaks resulting from the passage of the incident shock S, and the PC. The following fluctuations are as a result of the Mach waves generated by the combustion cloud. The first peak (S') of T4 is due to the arrival of the diffracted shock followed by a short duration pressure plateau. The pressure continues to increase (indicated by RS) when the diffracted shock reflects from the ejector walls and crosses the nozzle centerline. The pressure gradually reduces due to the expansion of the flow.

The diffracted shocks collide with the walls of the ejector and undergo regular reflection. As the effective wedge angle between the shock and the ejector reduces, the reflection type transitions to Mach reflection indicated by the presence of the Mach stem in Fig. 5a. In the same figure, the vortex cores (denoted as v) have travelled twice the height of the uniform area channel downstream, with the PC arriving at the location of the cores. As the combustion products emerge from the nozzle they are drawn into the circulation of the two vortex cores (Figs. 5b and 5c). Also, in Fig. 5b the formation of a separation region (SR) can be observed in the converging portion of the nozzle. The SRs are due to the discharge of PC from the NONEL tube and their entrainment to the propagation of the PC through the nozzle's throat. The interaction between the vortex cores and PCs leads to the annihilation of the vortex cores. The high temperature and high viscosity of the PC account for rapid decay of the vortices [19]. In a previous case of nonreactive flow, carried out by Zare-Behtash and Kontis [20], the vortex decay was through the shock–vortex interactions and diffusion of rotational energy to put surrounding fluid in motion. The decay of the vortices was slower in the nonreactive study, taking 420 μs from the time when the first detonation wave or shock enters the test section, as opposed to 344 μs for the reactive case.

The PC continue to move into the upper and lower atria of the nozzle while at the same time moving further into the ejector segment (Fig. 5d). The recirculation region continues to grow through Figs. 5c and 5d. The PC fill the upper and lower atria of the nozzle, as shown in Fig. 6 by the line. As the combustion products move further into the atria (Figs. 6a and 6b), the pressure builds up. However, the compression in the atria finally overcomes the momentum of the flow pushing the combustion products further in. This pushes the PC back into the center of the nozzle, as seen by the reduced height of the marker in Fig. 6c. The pressure trace of Fig. 7, which is for the transducer located on the top right-hand side (see Fig. 1), shows the compression (A) and the consequent expansion (B) of the flow.

As mentioned in Sec. I, ejectors are fluid pumps that are used to entrain secondary flows using a primary flow leading to

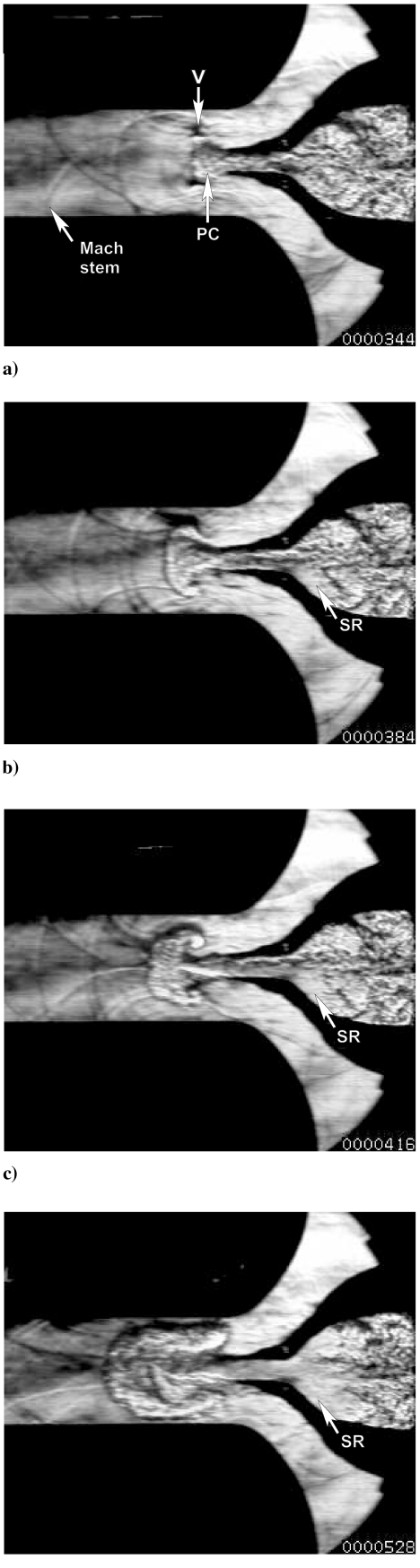

Fig. 5 Segment 2 of flow analysis.

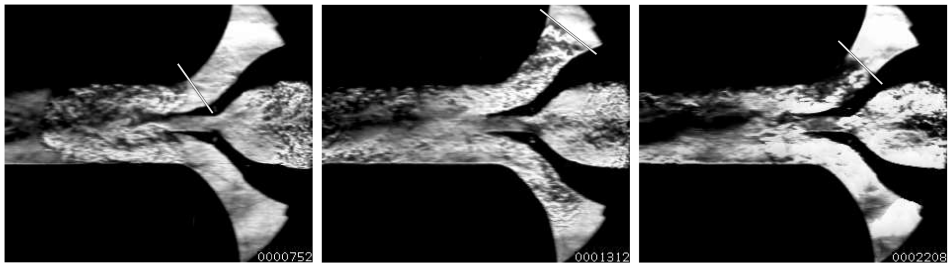

a) b) c)

Fig. 6 Segment 3 of flow analysis.

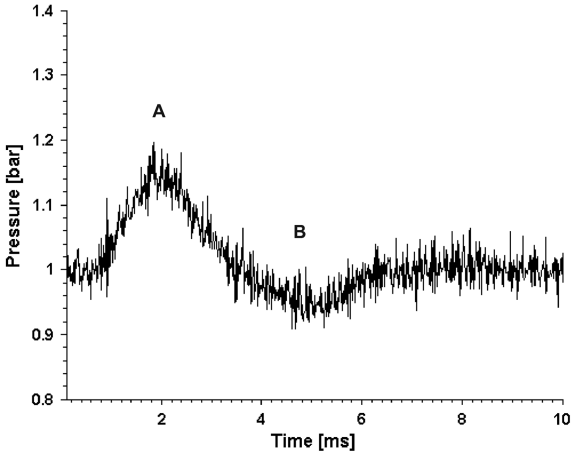

Fig. 7 Pressure trace of transducer T5.

augmentation of thrust. However, in this study the atria , which provide the inlet of secondary flow, were closed. The reason behind this chose was to study the physical features of the primary flow on the ejector. Further studies on the interaction of the secondary flows with the primary flows will be carried out in the near future.

IV. Conclusions

Using a nonelectrical (NONEL) tube with a combination of HMX and aluminum powder reactants deposited on the internal surface, a controlled and repeatable detonation was produced inside a 2-D nozzle-ejector system. Effects of 3-D flow at the initial stage of the detonation affect the incident shock front and the reflected shock wave system at the nozzle entrance. However, these effects are confined to the entrance by the area reduction due to the throat of the nozzle.

The incident shock wave generated within the NONEL tube travels through the test section unaffected by the PC which emerge from the tube. The diffraction of this shock generates two vortex cores due to the roll up of the shear layer at the nozzle exit. A secondary shock wave forms from the coalescence and strengthening of the Mach waves (produced from the combustion cloud) moving through the converging nozzle. This led to a second diffracted shock wave.

The interaction between the PC and the vortex cores leads to the annihilation of the vortices and the filling of the ejector section with combustion products. The combustion products continue to fill the test section cavities until the compression force overcomes the momentum of the flow and pushes the combustion products out from the cavities. Hence, the importance of entrainment of secondary flow to the ejector to avoid any loss of momentum by the escape of the flow through the atria.

Acknowledgments

The authors are grateful to the staff at the School of Mechanical, Aerospace, and Civil Engineering and to the Engineering and Physical Sciences Research Council engineering equipment loan pool for the loan of the Shimadzu system.

References

[1] Papalexandris, M. V., Thomas, J. F., Jacobs, C., and Deledicque, V., "Structural Characteristics of Detonation Expansion from a Small Channel to a Larger One," *Proceedings of the Combustion Institute*, Elsevier, New York, 2007, pp. 2407–2414.

[2] Ma, F., Choi, J. Y., and Yang, V., "Thrust Chamber Dynamics and Propulsive Performance of Single-Tube Pulse Detonation Engines," *Journal of Propulsion and Power*, Vol. 21, No. 3, 2005, pp. 512–526. doi:10.2514/1.7393

[3] Oh, J. Y., Ma, F., Hsieh, S. Y., and Yang, V., "Interactions Between Shock and Acoustic Waves in a Supersonic Inlet Diffuser," *Journal of Propulsion and Power*, Vol. 21, No. 3, 2005, pp. 486–495. doi:10.2514/1.9671

[4] Ohyagi, S., Obara, T., Hoshi, S., Cai, P., and Yoshihashi, T., "Diffraction and Re-Initiation of Detonations Behind a Backward-Facing Step," *Shock Waves*, Vol. 12, No. 3, 2002, pp. 221–226. doi:10.1007/s00193-002-0156-z

[5] Wilson, J., Sgondea, A., Paxson, D. E., and Rosenthal, B. N., "Parametric Investigation of Thrust Augmentation by Ejectors on a Pulsed Detonation Tube," *Journal of Propulsion and Power*, Vol. 23, No. 1, 2007, pp. 108–115. doi:10.2514/1.19670

[6] Glaser, A. J., Caldwell, N., Gutmark, E., Hoke, J., Bradley, R., and Schauer, F., "Study on the Operation of Pulse-Detonation Engine-Driven Ejector," *Journal of Propulsion and Power*, Vol. 24, No. 6, 2008, pp. 1324–1331. doi:10.2514/1.37869

[7] Etele, J., Parent, B., and Sislian, J. P., "Analysis of Increased Compression Through Area Constriction on Ejector-Rocket Performance," *Journal of Spacecraft and Rockets*, Vol. 44, No. 2, 2007, pp. 355–364. doi:10.2514/1.26915

[8] Alperin, M., and Wu, J. J., "Recent Development of a Jet-Diffuser Ejector," *Journal of Aircraft*, Vol. 18, No. 12, 1981, pp. 1011–1017. doi:10.2514/3.57594

[9] Alperin, M., and Wu, J. J., "Thrust Augmenting Ejectors, Part 1," *AIAA Journal*, Vol. 21, No. 10, 1983, pp. 1428–1436. doi:10.2514/3.60148

[10] Kentfield, J. A. C., "Fundamentals of Idealised Airbreathing Pulse-Detonation Engines," *Journal of Propulsion and Power*, Vol. 18, No. 1, 2002, pp. 77–83. doi:10.2514/2.5900

[11] Etele, J., Sislian, J. P., and Parent, B., "Effect of Rocket Exhaust Configuration on Ejector Performance in RBCC Engines," *Journal of Propulsion and Power*, Vol. 21, No. 4, 2005, pp. 656–666. doi:10.2514/1.10794

[12] Allgood, D., Gutmark, E., Rasheed, A., and Dean, A. J., "Experimental Investigation of a Pulse Detonation Engine with a Two-Dimensional Ejector," *AIAA Journal*, Vol. 43, No. 2, 2005, pp. 390–398. doi:10.2514/1.8125

[13] Ma, F., Choi, J.-Y., and Yang, V., "Propulsive Performance of Airbreathing Pulse Detonation Engines," *Journal of Propulsion and Power*, Vol. 22, No. 6, 2006, pp. 1188–1203.doi:10.2514/1.21755

[14] Yang, L. C., and Do, I. H. P., "Nonelectrical Tube Explosive Transfer System," *AIAA Journal*, Vol. 38, No. 12, 2000, pp. 2260–2267. doi:10.2514/2.917

[15] Eustace, V. A., "A Study of Two-Dimensional Supersonic Air Ejector Systems," Ph.D. Thesis, Univ. of Manchester Inst. of Science and Technology, Manchester, England, U.K., 1969.

[16] Oommen, C., Jagadeesh, G., and Raghunandan, B. N., "Studies on Microexplosive Driven Blast Wave Propagation in Confined Domains Using NONEL Tubes," *26th International Symposium on Shock Waves*, Springer, New York, 15–20 July 2007.

[17] Settles, G. S., *Schlieren and Shadowgraph Techniques*, Springer–Verlag, New York, 2001.

[18] Kontis, K., An, R., Zare-Behtash, H., and Kounadis, D., "Head-On Collision of Shock Wave Induced Vortices with Solid and Perforated Walls," *Physics of Fluids*, Vol. 20, 2008, Paper 016104. doi:10.1063/1.2837172

[19] Renard, P. H., Thevenin, D., Rolon, J. C., and Candel, S., "Dynamics of Flame/Vortex Interactions," *Progress in Energy and Combustion Science*, Vol. 26, No. 3, 2000, pp. 225–282. doi:10.1016/S0360-1285(00)00002-2

[20] Zare-Behtash, H., and Kontis, K., "Compressible Flow Structures Interaction with Two-Dimensional Ejector: A Cold-Flow Study," *Journal of Propulsion and Power*, Vol. 25, No. 3, 2009, pp. 707–716. doi:10.2514/1.39315

J. Powers
Associate Editor